Separation Science and Technology
Publication details, including instructions for authors and subscription information:
http://www.informaworld.com/smpp/title~content=t713708471

Effect of PAC Addition on the Physicochemical Characteristics of Bio-Cake in a Membrane Bioreactor

Woo-Nyoung Lee[a]; Kyung-Min Yeon[a]; Byung-Kook Hwang[a]; Chung-Hak Lee[a]; In-Soung Chang[b]
[a] School of Chemical and Biological Engineering, Seoul National University, Seoul, Korea [b] Department of Environmental Engineering, Hoseo University, Asan, Korea

Online publication date: 23 April 2010

To cite this Article Lee, Woo-Nyoung , Yeon, Kyung-Min , Hwang, Byung-Kook , Lee, Chung-Hak and Chang, In-Soung(2010) 'Effect of PAC Addition on the Physicochemical Characteristics of Bio-Cake in a Membrane Bioreactor', Separation Science and Technology, 45: 7, 896 — 903
To link to this Article: DOI: 10.1080/01496391003666999
URL: http://dx.doi.org/10.1080/01496391003666999

Separation Science and Technology, 45: 896–903, 2010

ISSN: 0149-6395 print/1520-5754 online
DOI: 10.1080/01496391003666999

Taylor & Francis
Taylor & Francis Group

Effect of PAC Addition on the Physicochemical Characteristics of Bio-Cake in a Membrane Bioreactor

Woo-Nyoung Lee,[1] Kyung-Min Yeon,[1] Byung-Kook Hwang,[1] Chung-Hak Lee,[1] and In-Soung Chang[2]

[1]*School of Chemical and Biological Engineering, Seoul National University, Seoul, Korea*
[2]*Department of Environmental Engineering, Hoseo University, Asan, Korea*

The effect of powdered activated carbon (PAC) addition on the architecture and cohesion strength of bio-cake in a membrane bioreactor (MBR) was investigated. Two reactors, a conventional MBR and a membrane-coupled biological activated carbon reactor (MBR_{ac}), were run in parallel. The addition of PAC led to a substantial increase in membrane permeability. Based on the conventional filtration theory, microbial floc size (d), bio-cake porosity (ϵ), and total attached biomass (TAB) were determined to find the key mechanism for the enhanced permeability. Unexpectedly the addition of PAC did not significantly change either the microbial floc size (d) or the porosity (ϵ) of the bio-cake. It decreased, however, not only the concentration of extra-cellular polymeric substances (EPS) in the bulk phase but also the TAB on the membrane. Using a separate batch cohesion test, it was revealed that the cohesion strength between microorganisms in the bio-cake in the MBR_{ac} was weaker than that in the MBR. The addition of PAC led to the reduction of EPS, which act as glue-like materials, which in turn weakened the cohesion strength of the microorganisms. This resulted in a lower amount of TAB, i.e., a smaller amount of the bio-cake on the membrane, which ultimately gave rise to the enhanced permeability in the MBR_{ac}.

Keywords adhesion strength; bio-cake; membrane bioreactor; porosity; powdered activated carbon

INTRODUCTION

Although a membrane bioreactor (MBR) for wastewater treatment is an attractive process with several advantages over a conventional bioreactor, the commercialization of MBRs has been constrained by membrane biofouling during the filtration of mixed liquor suspended solids (1,2). Therefore, during the last two decades many efforts have been made to reduce membrane biofouling in the MBR through backwashing (3), aeration (4), intermittent suction (5), module modification (6,7), and the addition of organic or inorganic additives (8–13).

Received 1 November 2009; accepted 31 December 2009.
Address correspondence to Chung-Hak Lee, School of Chemical and Biological Engineering, Seoul National University, Seoul 151-744, Republic of Korea. Tel.: +82-2-880-7075; Fax: +82-2-874-0896. E-mail: leech@snu.ac.kr

Powdered activated carbon (PAC) has been added to MBRs to mitigate membrane fouling because PAC is thought to remove low molecular weight organic foulants by adsorption (10–15). Studies have mainly focused on the enhancement of membrane permeability following the addition of PAC, but the influence of PAC on the physicochemical characteristics of bio-cake has not been taken into account in relation to the effect on permeability. Although some researchers reported that the cake layer formed in the membrane-coupled biological activated carbon reactor (MBR_{ac}) maintained higher porosity than that in a conventional MBR, they only estimated the cake porosity in the MBR_{ac} using a model equation, or calculated it indirectly from specific cake resistance without any direct measurement of cake porosity (16,17).

Therefore, in this study, we directly measured the bio-cake porosity in the MBR_{ac} using CLSM and image analysis techniques and investigated the effects of PAC addition on the physicochemical characteristics of the bio-cake, particularly the porosity and cohesion strength. Among the various techniques to evaluate biofilm structure, confocal laser scanning microscopy (CLSM) was used for the visualization of bio-cake layer and quantification of its porosity because CLSM is a powerful and reliable tool for the architectural analysis of the bio-cake formed on the membrane when combined with image analysis techniques (18).

MATERIALS AND METHODS

MBR Set-Up

Figure 1 shows a schematic of the experimental setup and Table 1 lists its operating conditions. To investigate the effect of PAC addition on MBR performance, two MBRs, a conventional MBR and MBR_{ac}, were run in parallel under the same operating conditions except for the addition of PAC into the MBR_{ac}. Compressed air (air flow rate = 1 L/min) was supplied through a bubble stone at the bottom of each reactor to provide dissolved oxygen and turbulence for mixing. Each reactor had a working volume of 2 liters.

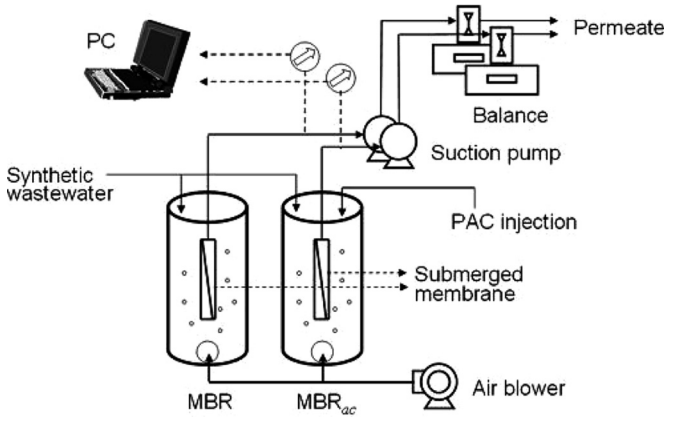

FIG. 1. Schematic diagram of a MBR system.

HRT and SRT were maintained at 10 hr and 30 days, respectively. The main carbon and nitrogen sources in the synthetic wastewater were glucose and ammonium sulfate.

An I-shaped hollow fiber membrane module (Fig. 2), made of PVDF (ZeeWeed 500, Zenon) with a pore size of 0.04 μm and a surface area of 200 cm^2, was dipped into each MBR. The permeate, through the submerged membrane, module was continuously withdrawn using a peristaltic pump at a constant flux of 15 $L/m^2 \cdot hr$. Trans-membrane pressure (TMP), an indicator of the extent of membrane fouling, was continuously monitored and the operation was stopped when the TMP reached 30 kPa because it was difficult to maintain a constant flux when TMP exceeds 30 kPa.

Powdered Activated Carbon

The specifications of the PAC (WPH, Calgon) used are listed in Table 2. PAC was sieved (200 × 500 mesh) and rinsed with DI water several times to remove impurities such as ashes. It was dried overnight at 110°C, and then stored in a desiccator. The mean particle size of PAC was measured several times and was around 44 μm in a slurry state.

TABLE 1
Operating conditions for the MBR and MBR$_{ac}$

	MBR	MBR$_{ac}$
Working volume (L)	2	
TMP (kPa)	<30	
Suction flux ($L/m^2 \cdot hr$)	15	
Air flow rate (L/min)	1	
DO (mg O_2/L)	>4	
pH	6.5 ~ 7.5	
Feed concentration (mg COD/L)	300 (±10)	
HRT (hr)	10	
SRT (day)	30	
MLSS (mg/L)	4,800 (±200)	5,100 (±200)
PAC dosage[a] (g/g MLSS)	non	0.1

[a]PAC was dosed one time per day right after sludge withdrawal.
( ): Standard deviation ($n = 10$).

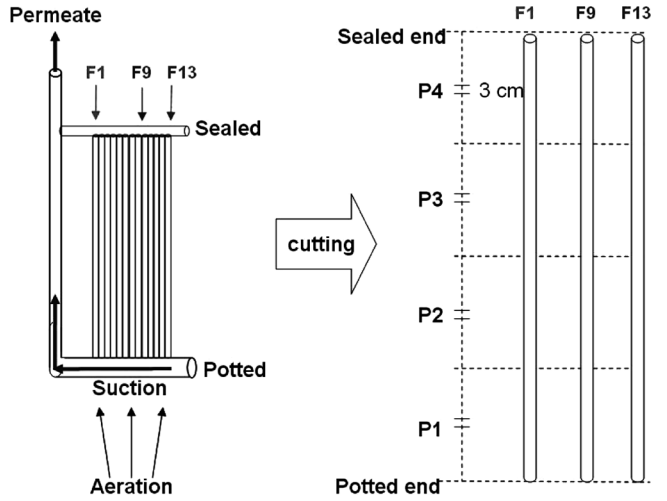

FIG. 2. The hollow fiber module and sampling points for the bio-cake specimens.

The activated sludge obtained from a local municipal wastewater treatment plant (Tancheon, Seoul, Korea) was acclimated and incubated in synthetic wastewater for one month prior to the filtration experiments. The MBR$_{ac}$ sludge was formed by adding PAC to the bioreactor intermittently. Membrane filtration, i.e., permeate withdrawal, started after two months' operation of the activated sludge reactor with PAC. The addition of PAC resulted in a higher concentration of mixed liquor suspended solids (MLSS) in the MBR$_{ac}$ than in the conventional MBR because the MLSS in the MBR$_{ac}$ contained the added PAC.

Analysis of Bio-Cake Architecture

When the TMP reached 30 kPa at Point 1 and 3 in Fig. 5, the membrane module was withdrawn from the MBR to measure the local porosities of the bio-cake. In Fig. 2, F1 to F13 indicate the horizontal locations of thirteen hollow fibers in the membrane module. Of these, three fibers (F1, F9, and F13) were cut, and each one was further cut into

TABLE 2
Specifications of PAC (WPH, Calgon)

Iodine number	min. 800
Moisture (mass-%)	max. 8
Specific surface area (m^2/g)	1,057
Ash content (mass-%)	7
Mean particle size (μm)	44

TABLE 3
Fluorescence probes used in bio-cake staining and their spectral characteristics

Probes	Label	Excitation (nm)	Emission (nm)	Specificity (target)	Channel
SYTO9	–	488	515/30	Nucleic acids (Bacterial cell)	Green
Concanavalin A	TRITC[a]	568	600/50	α-Mannose, α-glucose (Polysaccharide)	Red

[a]TRITC, tetramethylrhodamine isothiocyanate.

four segments (P1 ~ P4) of 3 cm each. P1 ~ P4 indicate the vertical location of each segment. Accordingly, twelve specimens (=3 fibers × 4 specimens/fiber) were obtained for staining and CLSM in total. The smaller the numbers of F and P indicates the closer the segment to the suction pump. Consequently, [F1, P1] indicates the nearest segment to the suction pump whereas [F13, P4] is located at the farthest point from the pump.

Cells and polysaccharides in the bio-cake were stained with SYTO9 and Concanavalin A (Molecular Probes, Eugene, USA), which are specific to nucleic acids and polysaccharides, respectively. The list of fluorescent dyes used in the bio-cake staining is given in Table 3. After the addition of dye, the bio-cake was incubated for 30 min at room temperature in the dark and then washed with a phosphate buffered saline (PBS) solution. The stained bio-cake was immediately observed by means of a CLSM system (Radiance 2000, Bio-Rad, UK) which consists of a microscope (Nikon, Japan) and a krypton-argon mixed gas laser source. Signals were recorded in the green (excitation = 488 nm, emission = 515/30 nm) and the red channels (excitation = 568 nm, emission = 600/50 nm). An oil lens (40 × 1.3 NA lens) was used for observations (magnification × 600). A series of CLSM images of optical sections with a step size of 1 μm were simultaneously taken for each specimen. Two CLSM images based on cells and polysaccharides, respectively, were merged together using the IMARIS Program (v 4.1.3, Bitplane AG, Zurich, Switzerland) (19) and then the merged images were used to calculate the porosity of the bio-cake with the software Image Structure Analyzer-2 (ISA-2), developed by Beyenal et al. (20).

Modification of CLSM Images

Unlike the bio-cake in the MBR, the bio-cakes formed in the MBR_{ac} contained PAC particles as well as microbial flocs because the PAC particles were able to attach to or intermingle with microbial flocs in the bulk phase. Those conjugated PAC and microbial flocs formed the bio-cake on the membrane surface as the filtration proceeded. On the CLSM image of the biocake in MBR_{ac}, PAC particles may be regarded as voids because they do not emit fluorescence even though they occupy a portion of the bio-cake layer. As shown in Fig. 3a, CLSM images of the biocake in the MBR_{ac} showed round-shaped voids (black spots marked with dotted circles) which were actually images representing the PAC. Therefore, the CLSM images of the bio-cake in the MBR_{ac} were modified using an image processing program (Adobe Photoshop 7.0). To fill up the voids formed by the PAC, cell images (green color) that had a similar area to the voids were copied and pasted onto the voids. As a result, the voids formed by the PAC particles were substituted by the cell images as shown in Fig. 3b. Based on the modified CLSM images, the real porosity of the bio-cake in the MBR_{ac} was determined using the ISA-2 software.

MBR with Latex Beads

Latex beads were substituted for the PAC to confirm the validity of the modification method for the CLSM images for determination of bio-cake porosity in the MBR_{ac}. The beads (Sigma L4530, carboxylate modified polystyrene, 2.5 wt%, USA) are mono-dispersed particles with a diameter of 2 μm and emit yellow-green fluorescence when exposed to laser light (excitation/emission = 470/550 nm). Instead of the PAC, the latex beads were added to the MBR on the right (Fig. 1) at a concentration of 0.1 mg/mg MLSS. Both the MBR with beads (on the right) and the MBR without beads (on the left) had a working

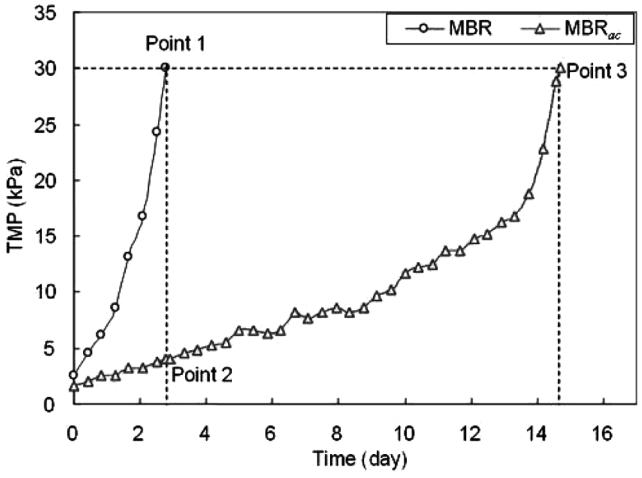

FIG. 3. Comparison of TMP increase between MBR and MBR_{ac}.

volume of 1 L. Both MBRs were run in parallel under the same operating conditions without sludge withdrawal at the HRT of 10 hr. Compressed air (air flow rate = 0.5 L/min) was supplied through a bubble stone on the bottom of each reactor, and an I-shaped PVDF membrane module (surface area = 100 cm^2) was dipped into each reactor. When the TMP reached 30 kPa, the membrane module was removed from each MBR to measure the bio-cake porosity. The membrane module had eight hollow fibers in total, and a 3-cm section in the middle of each fiber was removed to measure the bio-cake porosity.

Evaluation of Cohesion Strength of the Microbial Flocs in the Bio-Cake

To measure the cohesion strength of the microbial flocs in the bio-cake, a special experimental setup was designed (Fig. 4). A portion of mixed liquor equivalent to 250 mg MLSS was sampled from each reactor and was filtered through a 0.45-μm disc filter (Millipore, USA). The retained MLSS on the disc filter was placed on the bottom of a beaker with 1 liter of de-ionized water at 25°C. Then the beaker was placed in the Jar Tester (C-JT, Changshin Scientific Co., Ltd., Korea) at 100 rpm ($G = 340\ s^{-1}$) to maintain the same mixing intensity as that in the MBR and then the turbidity of the bulk solution in the beaker was monitored at a given time interval. Although the material and shape of the 0.45-μm disc filter were different from those of the hollow fiber membrane used in the MBR (Fig. 1), those differences would not affect substantially the results of the cohesion test because the most important parameter in the cohesion test is not the interaction between the cells and membrane surface but between the cells in the cake layer. Likewise, the difference in mixing devices between the stirrer in the beaker and aeration in the MBR would not break the rationality of the cohesion test.

Analytical Methods

Mixed liquor suspended solids (MLSS) were measured according to the analytical methods described in the Standard Methods (21). DO concentration and the pH of the mixed liquor were measured with a multimeter (Orion 1230, USA). COD was determined by a spectrophotometric method (DR 4000, HACH, U.S.A.). Particle size distributions were analyzed using a particle size analyzer based on a laser scattering method (Mastersizer/E, Malvern, UK) which allows the measurement of particle size in the range of $0.1 \sim 600$ μm.

To measure the total attached biomass (TAB) on the membrane surface, the membrane module was taken out of each reactor when the TMP reached 30 kPa, and repeatedly washed with a saline solution until more than 99% of biomass was detached from the membrane into the saline solution. The extraction of the bound EPS from the suspended microbial flocs was carried out using a heating method (6). Proteins and polysaccharides were analyzed by spectrophotometric methods: protein concentration was determined based on the modified Lowry method using the Lowry reagent (P 5656, Sigma). A calibration curve was prepared using a solution of bovine serum albumin as a standard. Polysaccharide concentration was determined using the phenol-sulfuric acid method with glucose as a standard (22).

RESULTS AND DISCUSSION

Effect of PAC Addition on Membrane Permeability

The rate of increase of TMP is an important factor when evaluating membrane permeability in a submerged MBR because it is directly related to membrane biofouling or permeability. TMP profiles as a function of time were monitored in the MBR and MBR_{ac} and compared as shown in Fig. 5. The TMP reached 30 kPa within 14.5 days in the MBR_{ac}, whereas only 2.7 days were required to reach the

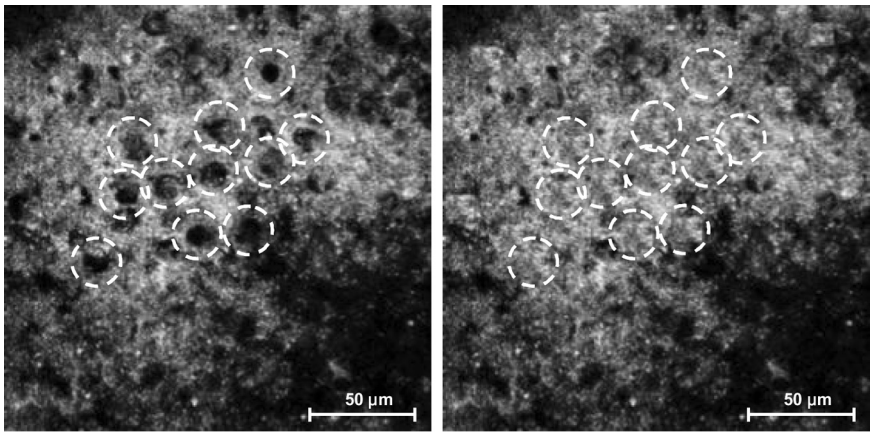

(a) (b)

FIG. 4. Modification of CLSM image acquired from MBR_{ac} bio-cake (×600).

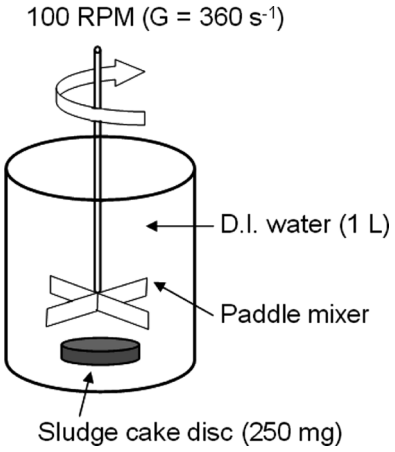

FIG. 5. Experimental setup for the evaluation of adhesion strength of activated sludge.

same TMP in the MBR, indicating that the rate of membrane biofouling in the MBR was more than five times faster than that in the MBR_{ac}. In other words, the addition of PAC to the MBR mitigated the membrane biofouling substantially, as reported elsewhere (16,17).

The conventional filtration theory tells us information about the correlation between the permeate flux and bio-cake properties, which is governed by its mass and specific resistance. It is expressed as follows (25):

$$J = \frac{\Delta P}{(R_m + R_c) \cdot \eta} \quad (1)$$

$$Rc = \alpha \cdot mc/A \quad (2)$$

where J is the flux, ΔP is the transmembrane pressure (TMP), R_m is the membrane resistance, R_c is the bio-cake resistance, m_c is the mass of the bio-cake, α is the specific bio-cake resistance and A is the membrane area.

It suggests that under the constant flux (J) operation in an MBR, the ΔP (TMP) is inversely proportional to the mass of the bio-cake (m_c) and the specific cake resistance (α), which is in turn inversely proportional to the particle size (d) and the porosity of the bio-cake (ϵ). In this context, we measured those three parameters (m_c, d, and ϵ) one by one in the MBR and MBR_{ac}, respectively, and compared them to elucidate the mechanism causing the difference in the increase in TMP between the two MBRs, as shown in Fig. 5.

Effect of PAC Addition on Microbial Floc Size

It is widely recognized that membrane permeability is closely related to the microbial floc size (d) and the concentration of soluble foulants including soluble organics and EPS in bulk solutions (2,23,24). Thus the floc size, soluble COD, and soluble EPS concentration in the bulk phase in both MBRs were determined to find the key factors mitigating the biofouling in the MBR_{ac}. As shown in Table 4, the enhanced membrane permeability of the MBR_{ac} could not be attributed to the differences in floc size (d) because the mean microbial floc sizes were similar to each other. In contrast, the soluble COD and EPS concentrations in the MBR_{ac} were lower than those in the MBR, which might be attributed to the adsorption of soluble organics by PAC (11,16). Therefore, a further study on the architecture (m_c and ϵ) of the bio-cake as well as EPS was necessary to fully explain the enhanced membrane permeability induced by PAC.

TABLE 4
Comparison of parameters affecting the membrane biofouling between the MBR and MBR_{ac}

	MBR	MBR_{ac}
Mean microfloc size (μm)	65 (±5)	62 (±7)
Soluble COD (mg/L)	21.3 (±2.1)	12.6 (±2.5)
Soluble EPS (mg/L)	8.4 (±1.1)	5.2 (±1.6)

( ): Standard deviation ($n = 10$).

Effect of PAC Addition on Bio-Cake Porosity

Figure 6 shows the distribution of the porosity of the bio-cakes at different vertical (S1 ~ S4) and horizontal (F1 ~ F13) positions on the membrane module. The bio-cake specimens sampled at Point 1 and 3 in Fig. 5. The porosity was largely dependent upon the location of the bio-cake over the module. In the vertical direction on the same fiber, the porosity near the potted end [S1] was lower than that near the sealed end [S4] for all fibers tested. In the horizontal direction, the porosity was always lower closer to the suction pump [F1] than that farther away [F9 and F13]. This can be attributed to the difference in the TMPs developed by the suction pump according to the horizontal and vertical positions of the bio-cakes over the membrane module. Lee et al. (26) reported that in a submerged MBR operating at constant flux, TMP gradually decreased and thus the bio-cake was less compressed as the distance of the bio-cake on a single fiber from the suction pump increased, which resulted in greater porosity.

With regard to the differences in the bio-cake porosities between the MBR and the MBR_{ac}, unexpectedly they were not significant at all positions over the membrane module (Fig. 6). This suggests that the addition of PAC to the MBR did not significantly change the bio-cake porosity itself. Some studies reported that the addition of PAC increased the bio-cake porosity (16,17). However, they only estimated the relative ratio of the bio-cake porosities (ϵ) in both reactors using the Carman Kozeny equation (25), and the average size of the bio-cake in each reactor, without direct measurement of ϵ.

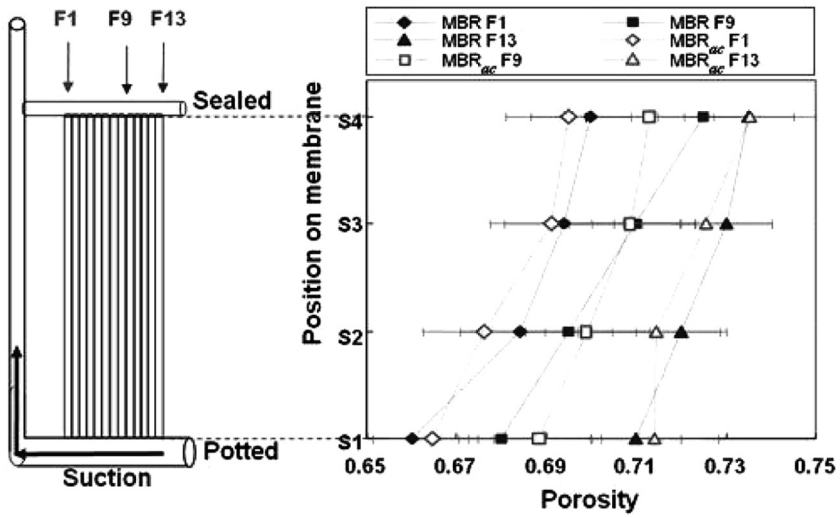

FIG. 6. Comparison of bio-cake porosity between MBR and MBR$_{ac}$.

As the image modification carried out using the Photoshop program in order to determine the bio-cake porosity in the MBR$_{ac}$ in this study is a somewhat artificial manipulation, it was necessary to confirm the validity of such modification of CLSM images. Fluorescence latex beads were thus substituted for the PAC to determine the effect of added solid particles on the porosity of the bio-cake in the MBR. As the latex beads emit yellow-green fluorescence when they are exposed to laser light, the void-error for the bio-cake with PAC was eliminated. Figure 7 shows the CLSM images acquired from the MBR without latex beads (Fig. 7a) and the MBR with latex beads (Fig. 7b). The latex beads and microbial cells were clearly differentiated from each other (Fig. 7b). For both MBRs with and without latex, the porosities were found to be similar to each other at all locations (Table 5). In other words, the addition of latex beads did not significantly affect the porosity of the bio-cake, confirming the validity of the image modification technique used to assess the bio-cake in the MBR$_{ac}$.

In summary, the addition of PAC did not substantially change the bio-cake porosity. Consequently, since the two parameters, d and ϵ were similar to each other for both MBRs, the search for the predominant mechanism for the enhanced permeability in the MBR$_{ac}$ turned to the third parameter, the mass of the bio-cake (m_c).

Amount of Total Attached Biomass

What was the key factor for the increase in membrane permeability in the MBR$_{ac}$? When the PAC was added to

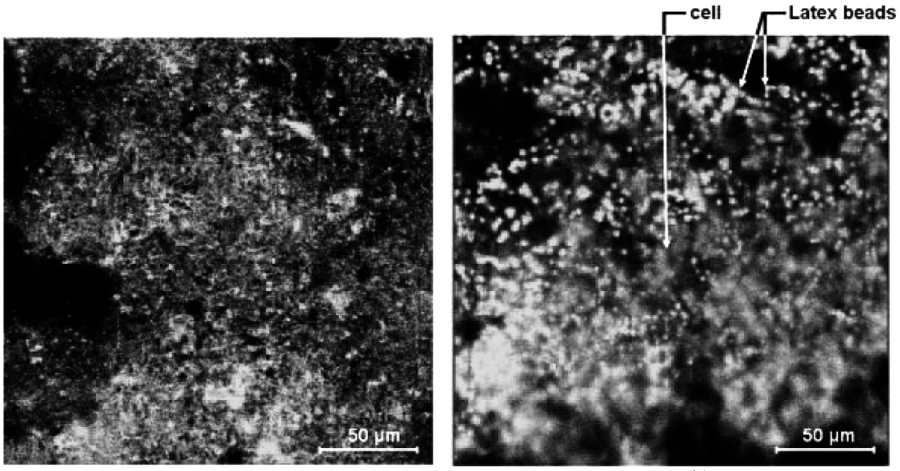

FIG. 7. CLSM images of MBR and latex bio-cake (×600).

TABLE 5
Comparison of the bio-cake porosity between the MBRs with and without latex beads

	MBR without latex	MBR with latex
Fiber 1′	0.67	0.66
Fiber 3′	0.73	0.74
Fiber 6′	0.74	0.74
Fiber 8′	0.75	0.78
Average	0.72 (±0.06)	0.73 (±0.06)

( ): Standard deviation ($n = 12$).

the MBR it removed sticky material like EPS as shown in Table 4 and thus the detachment of microbial flocs from the bio-cake layer into the bulk phase was facilitated, which might decrease the mass of the bio-cake (m_c) in the MBR_{ac}. Therefore, the amount of the total attached biomass (TAB) was measured in each MBR to compare the accumulation rate of bio-cake for both MBRs. The results are shown in Table 6.

At the same operation time of 2.7 days, the TAB amounted to 105 mg in the MBR but only 37 mg in the MBR_{ac} (Point 1 vs. 2 in Fig. 5). However, the TAB values were more similar at the same TMP of 30 kPa (Point 1 vs. 3 in Fig. 5). Consequently, it could be concluded that the TAB was in close association with the TMP and that the accumulation rate of the biomass in the MBR_{ac} was much slower than that in the MBR. Thus we investigated the attachment and/or detachment mechanisms of the biomass to/from the bio-cake layer in more detail.

The build-up of biomass in the bio-cake might be limited by the lack of EPS because the EPS is known to act like a glue connecting cells to each other. Therefore, if a portion of EPS had been removed by the PAC, the accumulation or build-up of the biomass (m_c) to form the bio-cake would have been much more retarded in the MBR_{ac} than in the PAC-free environment. This might be explained by the cohesion strength of microbial flocs, which refers to the strength required for the formation of the microbial flocs. Therefore it was necessary to compare the cohesion strength of microbial flocs in the MBR with that in the MBR_a. As the detachment rate of TAB from the bio-cake

TABLE 6
Comparison of total attached biomass between the MBR and MBR_{ac}

	Control	MBR_{ac}	
	Point 1	Point 2	Point 3
TAB[a] (mg)	105 (±15)	37 (±8)	112 (±21)

[a]TAB; total attached biomass ($n = 3$).

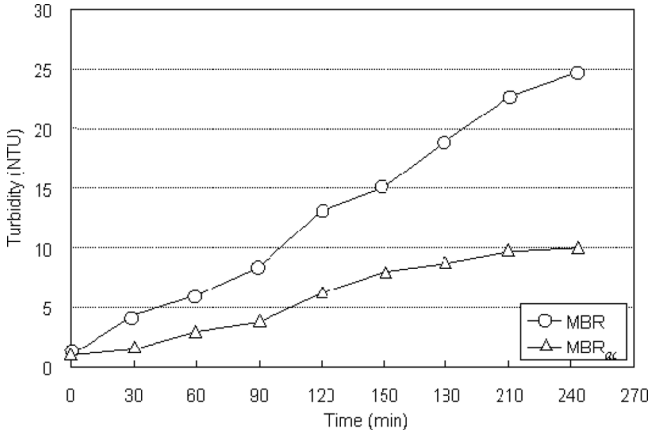

FIG. 8. Variations in turbidity in the evaluation of adhesion strength of mixed liquor.

into the bulk phase was assumed to be indirectly linked to the cohesion strength of the microbial flocs, the experiment was carried out as described in the section titled "Evaluation of Cohesion Strength of the Microbial Flocs in the Bio-Cake."

Figure 8 shows the variation in turbidity during the evaluation of the cohesion strength of the microbial flocs. The turbidity measured with the bio-cake disc from MBR_{ac} was about 2 to 3 times greater than that from the MBR at all time intervals, indicating that the microbial flocs in the MBR_{ac} had much lower cohesion strength than those in the MBR. Since the PAC could remove, albeit partially, the EPS that act as a glue and thus are necessary for the formation of the bio-cake as well as the microbial flocs, the microbial flocs in the MBR_{ac} would be detached more easily under the hydrodynamic shear stress caused by aeration. This may mitigate the rate of accumulation of the bio-cake on the membrane surface and ultimately reduce membrane biofouling.

CONCLUSIONS

The addition of PAC to the MBR resulted in a substantial increase in membrane permeability. To determine the main cause of the enhanced permeability, the effects of PAC on the architecture of the bio-cake and on the cohesion strength were investigated and the following conclusions can be drawn:

1. The addition of PAC did not significantly affect the microbial floc size (d) nor the porosity (ϵ) of the bio-cake in the MBR_{ac}.
2. The cohesion strength by which microorganisms in the bio-cake bind together became weaker in the MBR_{ac} than in the MBR. This was because the addition of PAC led to a reduction in EPS, which act as glue-like materials, which in turn weakened the cohesion strength of the microorganisms.

3. The weakened cohesion strength between microorganisms resulted in a lower amount of TAB, i.e., a smaller thickness of the bio-cake on the membrane under the shear stress generated by aeration, which ultimately gave rise to the enhanced permeability in the MBR_{ac}.

ACKNOWLEDGEMENTS

This work was supported by the Korea Science and Engineering Foundation (KOSEF) grant funded by the government (MOST) (No. R0A-2007-000-20073-0). Woongjin Chemical Co., Korea is appreciated for providing us with membrane modules used in this work. The authors thank the National Instrumentation Center for Environment Management (NICEM) for the use of the confocal laser scanning microscope system.

REFERENCES

1. Chang, I.S.; Clech, P.L.; Jefferson, B.; Judd, S. (2002) Membrane fouling in membrane bioreactors for wastewater treatment. *J. Environ. Eng.*, 128 (11): 1018.
2. Ramesh, A.; Lee, D.J.; Wang, M.L.; Hsu, J.P.; Juang, R.S.; Hwang, K.J.; Liu, J.C.; Tseng, S.J. (2006) Biofouling in membrane bioreactor. *Sep. Sci. and Technol.*, 41: 1345.
3. Visvanathan, C.; Yang, B.S.; Muttanmara, S.; Maythanukhraw, R. (1997) Application of air backflushing technique in membrane bioreactor. *Water Sci. Technol.*, 36 (12): 259.
4. Ueda, T.; Hata, K.; Kikuoka, Y.; Seino, O. (1997) Effects of aeration on suction pressure in a submerged membrane bioreactor. *Water Res.*, 31 (3): 489.
5. Yamamoto, K.; Hiasa, M.; Mahmood, T.; Matsuo, T. (1989) Direct solid-liquid separation using hollow fiber membrane in an activated sludge aeration tank. *Water Sci. Technol.*, 21 (4–5): 43.
6. Chang, I.S.; Lee, C.H. (1998) Membrane filtration characteristics in membrane coupled activated sludge system – The effect of physiological states of activated sludge on membrane fouling. *Desalination*, 120 (3): 221.
7. Yoon, S.H.; Kim, H.S.; Yeom, I.T. (2004) Optimization model of submerged hollow fiber membrane modules. *J. Membr. Sci.*, 234 (1–2): 147.
8. Lee, W.N.; Chang, I.S.; Hwang, B.K.; Park, P.K.; Lee, C.H.; Huang, X. (2007) Changes in biofilm architecture with addition of membrane fouling reducer in a membrane bioreactor. *Process Biochem.*, 42 (4): 655.
9. Lee, J.C.; Kim, J.S.; Kang, I.J.; Cho, M.H.; Park, P.K.; Lee, C.H. (2002) Potentials and limitation of alum or zeolite addition to improve the performance of submerged membrane bioreactor. *Water Sci. Technol.*, 43 (11): 59.
10. Ng, C.A.; Sun, D.; Fane, A.G. (2006) Operation of membrane bioreactor with powdered activated carbon addition. *Sep. Sci. and Technol.*, 41: 1447.
11. Kim, J.S.; Lee, C.H. (2003) Effect of powdered activated carbon on the performance of an aerobic membrane bioreactor: Comparison between cross-flow and submerged membrane system. *Water Environ. Res.*, 75 (4): 300.
12. Guo, W.S.; Vigneswaran, S.; Ngo, H.H.; Van Nguyen, T.B.; Ben Aim, R. (2006) Influence of bioreaction on a long-term operation of a submerged membrane adsorption hybrid system. *Desalination*, 191: 92.
13. Ying, Z.; Ping, G. (2006) Effect of powdered activated carbon dosage on retarding membrane fouling in MBR. *Sep. Purif. Technol.*, 52: 154.
14. Yun, M.A.; Yeon, K.M.; Park, J.S.; Lee, C.H.; Chun, J.; Lim, D.J. (2006) Characterization of biofilm structure and its effect on membrane permeability in MBR for dye wastewater treatment. *Water Res.*, 40 (1): 45.
15. Jin, Y.L.; Lee, W.N.; Lee, C.H.; Chang, I.S.; Huang, X.; Swaminathan, T. (2006) Effect of DO concentration on biofilm structure and membrane filterability in submerged membrane bioreactor. *Water Res.*, 40 (15): 2829.
16. Kim, J.S.; Lee, C.H.; Chun, H.D. (1998) Comparison of ultrafiltration characteristics between activated sludge and BAC sludge. *Water Res.*, 32 (11): 3443.
17. Li, Y.Z.; He, Y.L.; Liu, Y.H.; Yang, S.C.; Zhang, G.J. (2005) Comparison of the filtration characteristics between biological powdered activated carbon sludge and activated sludge in submerged membrane bioreactors. *Desalination*, 174: 305.
18. Park, P.K.; Lee, C.H.; Lee, S. (2007) Determination of cake porosity using image analysis in a coagulation-microfiltration system. *J. Membr. Sci.*, 293: 66.
19. Staudt, C.; Horn, H.; Hempel, D.C.; Neu, T.R. (2004) Volumetric measurements of bacterial cells and extracellular polymeric substance glycoconjugates in biofilm. *Biotechnol. Bioeng.*, 88 (5): 585.
20. Beyenal, H.; Donovan, C.; Lewandowski, Z.; Harkin, G. (2004) Three-dimensional biofilm structure quantification. *J. Microbiol. Methods*, 59: 395.
21. APHA, AWWA, WEF (2005) *Standard Methods for the Examination of Water and Wastewater.* 22nd ed.; American Public Health Association: Washington, DC.
22. Dubois, M.; Gilles, K.A.; Hamilton, J.K.; Rebers, P.A.; Smith, F. (1956) Colorimetric method for determination of sugars and related substances. *Anal. Chem.*, 28: 350.
23. Kim, J.S.; Lee, C.H.; Chang, I.S. (2001) Effect of pump shear on the performance of a crossflow membrane bioreactor. *Water Res.*, 35 (9): 2137.
24. Chen, M.-Y.; Lee, D.-J.; Tay, J.H. (2006) Extracellular Polymeric Substances in Fouling Layer. *Sep. Sci. and Technol.*, 41: 1467.
25. Baker, R.J.; Fane, A.G.; Fell, C.J.D.; Yoo, B.H. (1985) Factors affecting flux in crossflow filtration. *Desalination*, 53: 81.
26. Lee, W.N.; Hwang, B.K.; Yeon, K.M.; Lee, C.H.; Chang, I.S. (2008) Effect of powdered activated carbon on bio-cake structure in biological activated carbon-ultra filtration process for wastewater treatment, Biofilm Technologies 2008, IWA International Conference, Singapore.